Influence of disorder on the electronic structure of amorphous silicon*

Jasprit Singh†
James Franck Institute and Department of Physics, University of Chicago, Chicago, Illinois 60637
(Received 20 August 1980; revised manuscript received 19 November 1980)

We have examined the electronic structure of amorphous silicon using a tight-binding scheme with all first- and second-neighbor couplings in a continuous random network. Matrix elements and deformation potentials were taken from the crystalline band structure. The effect of bond-length and bond-angle variations is relatively small and contributes to the narrow tails at the band edges. The effect of dihedral-angle disorder was examined keeping only the nearest-neighbor interactions in the Hamiltonian. The dihedral-angle disorder was found to be important at the valence-band edge and responsible for the observed features near the top of the valence band. Topological disorder was found to have important consequences in the bulk of the bands as well as at the conduction-band edge. Apart from the effects of the bond-length and bond-angle disorder, the states at the band edges are confined within regions closely approaching the crystalline structure locally, where they have the same form as in the crystal, but do not extend through the entire structure.

I. INTRODUCTION

In recent years amorphous silicon (a-Si) has become an intensely studied material. One of the main reasons for this interest is the unusually low density of localized states achievable in the band gap.[1,2] These narrow localized tails make a-Si very interesting from the technological point of view. The low density of gap states allows a good effective mobility for the charged carriers. It is also possible to make junctions with deeply penetrating electric fields. Since a-Si is much cheaper to make than crystalline silicon, it becomes a good candidate for solar cells. It is very important, therefore, to understand theoretically the origin and nature of localized states, why the tails are narrow, and how narrow they can get.

The electronic structure of silicon changes substantially in going from the crystalline to the amorphous state. The crystalline density of states shows three main peaks in the valence band as shown in Fig. 1(a).[3,4] In going to the amorphous state, the results of photoemission experiments[3,4] indicate that the peak I is relatively unaffected while peaks II and III merge to form a broad hump as shown in Fig. 1(b). Peak I, when carefully examined, shows some interesting quantitative changes. It becomes asymmetrically tilted towards higher energy and its width narrows. These changes have to be contrasted with extremely narrow band-edge tails in amorphous films made by passing silane through a glow discharge chamber.[1] These films have a substantial hydrogen content, and the hydrogen seems to remove the coordination defects thus removing most of the defect-related gap states. The use of fluorine along with hydrogen has further reduced the gap states.[2] With the experimental techniques improving, it is conceivable that one may have films approaching ideality in structure with only intrinsic localized states, i.e., states arising from the disorder present in the amorphous structure and not from structural defects. It is thus important to study the amorphous structure without any defects. Such structures are known as ideal continuous random networks (CRN), and our work will be confined to these structures.

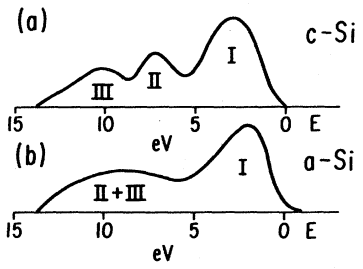

FIG. 1. (a) Density of states in the valence band of crystalline silicon. I, II, III denote the three peaks. (b) Density of states of the valence band of a-Si (XPS results).

Considerable effort has been made to understand the electronic structure of a-Si and other tetrahedral amorphous semiconductors. Weaire and Thorpe[5,6] have proved certain general theorems concerning the existence of well defined band edges for a very simple Hamiltonian. The disorder considered is topological, and only one of the four possible nearest-neighbor interactions is included. Numerical work using an extension of the Weaire-Thorpe model has been done by Kelly and Bullett.[7] Work has been also done by Ching, Lun, and Guttman[8] using various computer-generated CRN's. Joannopoulos and Cohen[9] have studied various crystalline forms of silicon and used the pseudopotential method to look at their band structures. Assuming that the amorphous

state will reflect the properties of the mixture of all these structures, they have concluded that bond-angle disorder and the presence of odd rings is very important. Joannopoulos[10] has used the cluster-Bethe-lattice method to study the effects of bond-angle and bond-length disorder using nearest-neighbor interactions. He found the former to be much more important than the latter. Ziman[11] has studied the edges of the valence band by assuming that the character of the wave functions there were of the same form as in the crystal. He concluded that the bottom of the valence band was little affected by disorder while the top was quite sensitive.

Here we examine the electronic structure of a-Si using a tight-binding scheme. A method to study the effect of quantitative disorder (due only to bond-angle and bond-length disorder) has already been reported.[12] In Sec. II we discuss this method briefly and give the results for quantitative disorder so as to compare them to the effects of dihedral-angle disorder and topological disorder. Section III deals with the importance of dihedral-angle disorder and in Sec. IV we develop a scheme to study the limits of the electron spectrum. Section V deals with the effect of dihedral-angle disorder on the valence-band states. In Sec. VI we deal with the effect of dihedral-angle disorder on the conduction-band edge and discuss the overall effect of quantitative disorder. In Sec. VII we discuss the total effect of quantitative disorder, and finally Sec. VIII deals with topological disorder. We conclude with Sec. IX.

II. EFFECT OF QUANTITATIVE DISORDER

In results reported earlier[12] it has been pointed out that quantitative disorder involving only bond-length and bond-angle disorder does not play a very important role in the electronic structure of silicon. We discuss here briefly the procedure for studying the effect of quantitative disorder and we set the basis for the following sections on dihedral-angle and topological disorder.

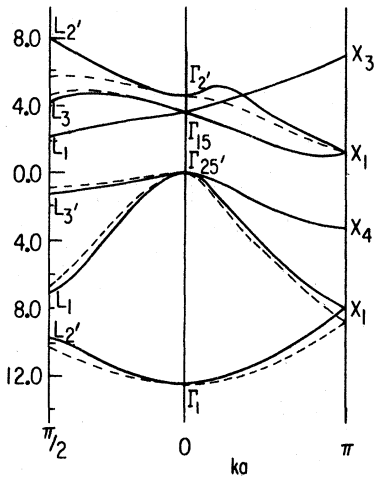

FIG. 2. Band structure of crystalline silicon. The dotted lines are the TB fit while the dark lines are the results of pseudopotential calculations.

A tight-binding fit is made using the Koster-Slater[13] method to a band structure calculated by pseudopotential theory.[14] This involves thirteen interaction terms since up to second-neighbor interactions are included. This gives a good fit (Fig. 2) for the valence band the lower 3.5 eV of the conduction band. The matrix elements required for the fit are shown in Table I. The notation is as used by Koster-Slater. Each element represents the interaction between the atomic orbital at (0, 0, 0) and the point in the parenthesis. The subscripts s, x, y, and z stand for the s, p_x, p_y, p_z functions.

In order to study the effects of quantitative disorder one needs to study the various models available for a-Si. Several models have been proposed for a continuous randon network (CRN).[15-17] The quantities characterizing a CRN are the bond-angle, bond-length, and dihedral-angle values. In addition the ring statistics is a very important

TABLE I. Tight-binding matrix elements for crystalline silicon.[a]

Matrix element	$E_{ss}(0)$	$E_{xx}(0)$	$E_{ss}(\frac{1}{2},\frac{1}{2},\frac{1}{2})$	$E_{xx}(\frac{1}{2},\frac{1}{2},\frac{1}{2})$	$E_{xy}(\frac{1}{2},\frac{1}{2},\frac{1}{2})$	$E_{sx}(\frac{1}{2},\frac{1}{2},\frac{1}{2})$	
Value in eV	−5.4	1.0	−2.05	0.43	1.20	1.13	
Matrix element	$E_{xx}(0,1,1)$	$E_{ss}(1,1,0)$	$E_{xx}(1,1,0)$	$E_{xy}(1,1,0)$	$E_{sx}(1,1,0)$	$E_{xy}(0,1,1)$	$E_{sx}(0,1,1)$
Value in eV	−0.25	0.11	0.21	0.07	0.03	0.0	0.03

[a]Note that the values given here are different from the misprinted values in M. H. Cohen, J. Singh, and F. Yonezawa, J. Non-Cryst. Solids 35–36, 55 (1980).

property of the CRN but will be discussed in Sec. VIII. Examination of the various models suggests that we choose the following characterizations for the structure. The bond-length variations about the crystalline value are Gaussian with an rms deviation $\Delta R/R = 0.015$. The bond angle θ varies about its mean value of 109.3° with an rms deviation of $\Delta\theta = 10°$. The dihedral angle is defined as the angle between the second-neighbor bonds when projected onto a plane perpendicular to the common bond as shown in Fig. 3. For the crystalline case the dihedral angle (ϕ) has a value of ±60°, 180° (staggered configuration), but in the amorphous state it varies as shown in Fig. 4. The distribution can be represented by the equation

$$P(\phi) = A(\tfrac{2}{3}\sin^2\tfrac{3}{2}\phi + \tfrac{1}{3}), \quad (1)$$

where A is a normalization constant. The maxima in $P(\phi)$ occur at the staggered configuration, $\phi = \pm 60°$, 180°, and the minima at the eclipsed configuration, $\phi = 0°$, ±120°.

To estimate the quantitative disorder we use the deformation-potential[18] theory and express it in our tight-binding scheme. Using the molecular approximation[13] and the results of modulation spectroscopy[19] we get the various deformation potentials. Once the deformation potentials are known, the effects of bond-length and bond-angle fluctuations equal to the rms values noted above can be found in a straightforward way.[12] Table II shows the fluctuations introduced at the band edges of silicon. Although a-Si is not deformed crystalline silicon, these numbers give a good estimate of the quantitative disorder.

As will appear in the following, the quantitative disorder introduced by the bond-length and bond-angle variation is relatively small compared to the dihedral-angle disorder effects and the effects of the topological disorder. Accordingly, in discussing the latter, we shall ignore the effects of bond-length and bond-angle disorder and give the matrix elements the values they have for the crystalline bond lengths and bond angles. We shall then discuss briefly how the results so obtained are modified by the bond-length and bond-angle variations.

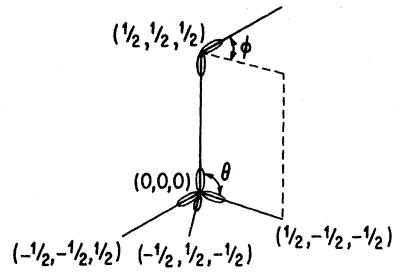

FIG. 3. Geometry of the diamond structure showing the bond angle θ and the dihedral angle ϕ.

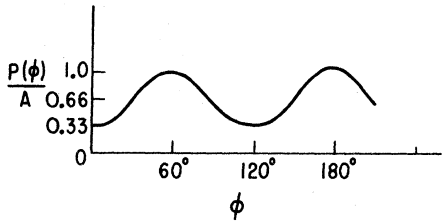

FIG. 4. Dihedral-angle distribution for CRN's taken from various models. $P(\phi)$: the probability distribution; A: normalization constant.

III. THE IMPORTANCE OF DIHEDRAL-ANGLE DISORDER

The dihedral angle has been defined in Sec. III and Fig. 3. Dihedral-angle disorder arises from random rotations around bonds, and the ease with which such rotations can be made accounts for the large fluctuations of the dihedral angle (Fig. 4). The dihedral-angle disorder does not alter the distances between atoms as it simply involves rotations about bonds. It is therefore not possible to see its effects by using the deformation-potential theory. To study the effects of the dihedral-angle variations, we need to extend the Weaire-Thorpe model[5] and explicitly study a structure-dependent Hamiltonian. Kelly and Bullett[7] studied a structure-dependent Hamiltonian, but not all nearest-neighbor interactions were included. We find that the complete Hamiltonian in fact makes the study easier and gives us insight into the amorphous state without having to employ numerical calculations.

To study the effect of dihedral-angle disorder it is convenient to use the sp^3 bond basis. In this representation the nearest-neighbor interactions are V_1 through V_6 as shown in Fig. 5. These are known in terms of the Koster-Slater interactions (Table I) by a simple transformation. For the crystalline case we put $\tilde{V}_4 = V_4$, $\tilde{V}_4' = V_5 = V_6$, and find that

$$V_1 = -1.6 \text{ eV}, \; V_2 = -4.3 \text{ eV}, \; V_3 = -0.38 \text{ eV}, \quad \tilde{V}_4 = 0.3 \text{ eV}, \; \tilde{V}_4' = -0.45 \text{ eV}. \quad (2)$$

TABLE II. Approximate changes produced in $\Gamma_{25'}$ and X_1 due to bond-length ($\Delta R/R = 0.015$) and bond-angle ($\Delta\theta = 10°$) variations.

Structural change	$\Delta\Gamma_{25'}$ (eV)	ΔX_1 (eV)
ΔR	0.02	0.025
$\Delta\theta$	0.2	0.15

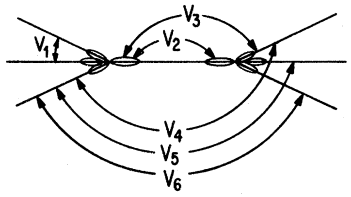

FIG. 5. On-site and nearest-neighbor interactions in the bond representation.

Clearly V_1 and V_2 are the strongest interactions, which is why the Weaire-Thorpe model is a good starting approximation. From Fig. 5 it is clear that V_1, V_2, V_3 are independent of dihedral-angle distributions. Thus by keeping only the V_2 and the V_3 term we can not study the dihedral-angle effects. The effect of dihedral-angle variations is manifested in the V_4, V_5, and V_6 terms. We define a convention shown in Fig. 6(a): V_4 is the interaction with the farthest bond, V_5 with the next farthest, and V_6 with the closest. It follows from this choice that $|V_4| < |V_5| \leq |V_6|$. All results have to be periodic in the dihedral angle ϕ with a period of 120°, as is clear from the rotation symmetry of the diamond structure. V_4, V_5, and V_6 as defined above are special cases of the general interaction $V(\phi)$ as displayed in Fig. 6(b). The dark line represents the bond connected to the (1, 1, 1) atom and the dotted line the bond connected to the (0, 0, 0) atom. Using the matrix elements from Table I, we find that

$$V(\phi) = 0.3 - 1.0\cos^2\phi/2 \qquad (3)$$

expressed in eV. There is a substantial variation in the interaction (~1 eV), and the dihedral-angle variations and therefore important for the electronic structure (Fig. 7).

We note, however, a very important invariance relation, viz.,

$$V_4 + V_5 + V_6 = \text{const}. \qquad (4)$$

This relation is especially useful when we study band limits and their dependence on dihedral-angle variation. An eigenvalue involving the combination $(V_4 + V_5 + V_6)$ will be an invariant under dihedral-angle fluctuations. Clearly it is important to include all nearest-neighbor interactions to realize this result. Looking more carefully at the invariants, viz., V_2, V_3 $(V_4 + V_5 + V_6)$, we find that all of these are made up of σ interactions, i.e., $ss\sigma, sp\sigma, pp\sigma$. The $pp\pi$ interaction is not an invariant under dihedral-angle rotations, as can be easily visualized.

The scale of variation of $V(\phi)$, ~1 eV, and the broad range of ϕ found in the structure force us to include dihedral-angle variation as a primary source of the effects of disorder on the electronic structure of a tetrahedral amorphous semiconductor.[20] The broad range of ϕ arises from the low restoring force for rotation around the bonding axis and is itself the ultimate source of the breakdown of the long-range order and of the topological disorder. Accordingly, we include topological disorder and dihedral-angle disorder on an equal footing in our discussion of the electronic structure.

IV. THE ELECTRONIC STRUCTURE

In this section we shall use the method of Weaire and Thorpe and extend it to a more complete Hamiltonian. The Hamiltonian can be written as

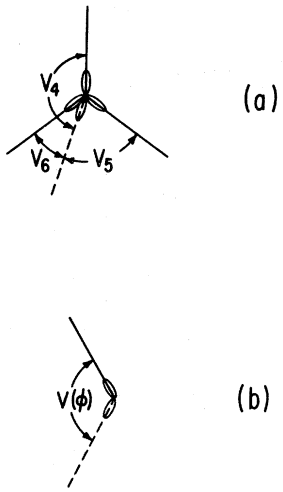

FIG. 6. (a) Convention for the dihedral-angle-dependent interactions. (b) A general dihedral-angle-dependent interaction.

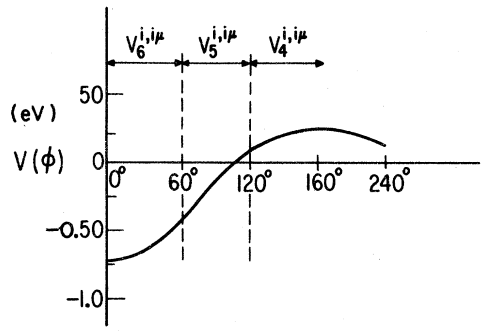

FIG. 7. Variation of $V(\phi)$ with dihedral angle. The ranges of the interactions V_4, V_5, and V_6 are shown for the disordered structure.

$$H=\sum_{i,\mu,\nu;\mu\neq\nu}|i\mu\rangle V_1\langle i\nu|+\sum_{i,\mu}|i\mu\rangle V_2\langle i_\mu\mu|+\sum_{i,\mu,\mu';\mu\neq\mu'}|i\mu\rangle V_3\langle i_\mu\mu'|+\sum_{i,\mu,\mu';\mu\neq\mu'}|i\mu\rangle V_\alpha^{i,i_{\mu'}}\langle i_\mu,\mu_\alpha|. \tag{5}$$

Here i denotes a site index and μ a bond index. Site i has a neighbor i_μ which is along the bond μ. A one-to-one correspondence exists between the bonds at site i and the bonds at site i_μ, which is used in the last three terms. The interactions V_α, $\alpha=4,5,6$ are now site dependent, and the bond indices appearing in these terms are defined by the convention discussed above.

It is important to realize that since we have included only nearest-neighbor interactions, an electron sees the same atomic configuration around itself at each site. This would not be so if the second-neighbor interactions had also been included. However, it is not just the immediate neighborhood which governs the nature of eigenstates as was realized by Cohen *et al.*[21] for the topologically disordered s-band structure and earlier by Joannopoulos and Cohen.[9] The immediate neighborhood defines the limits of the band spectra, while the global features determine whether or not certain states can exist on the entire structure.

We are primarily interested in the limits of the spectrum of this Hamiltonian and general features near those limits. We shall assume a wave function of the form

$$\psi=\sum_{i\mu}a_{i\mu}|i\mu\rangle,\ \sum_{i\mu}|a_{i\mu}|^2=1. \tag{6}$$

Using the variational principle we can then look at the limits of the energy spectrum. Using (6) in the Hamiltonian, we get for the energy

$$E=C_1V_1+C_2V_2+C_3V_3+\sum_\alpha E_\alpha, \tag{7}$$

where we have removed the restriction that V_1 couples different bonds on the same atom, and have included the self-interaction which only shifts the origin of energy. The various terms in (7) are

$$\begin{aligned}
C_1&=\sum_i\Big|\sum_\mu a_{i\mu}\Big|^2,\\
C_2&=\sum_{i\mu}a_{i\mu}^*a_{i_\mu\mu},\\
C_3&=\sum_{i\mu}a_{i\mu}^*D_{i_\mu}+\sum D_i^*a_{i_\mu\mu}-2C_2,\\
E_4&=\sum_{i,\mu,\mu';\mu\neq\mu'}a_{i\mu}^*a_{i_{\mu'}\mu_4}V_4^{i,i_{\mu'}},\\
E_5&=\sum_{i,\mu,\mu';\mu\neq\mu'}a_{i\mu}^*a_{i_{\mu'}\mu_5}V_5^{i,i_{\mu'}},\\
E_6&=\sum_{i,\mu,\mu';\mu\neq\mu'}a_{i\mu}^*a_{i_{\mu'}\mu_5}V_6^{i,i_{\mu'}},
\end{aligned} \tag{8}$$

where $D_i=\sum_\mu a_{i\mu}$. From the definitions of the $|i\mu\rangle$, $D_i=0$ means a pure p state. As discussed before, the problem of including only the V_1 and V_2 terms was solved by Weaire and Thorpe. We shall reconstruct their results and in the same spirit study the full Hamiltonian. The study of the terms becomes easy if we cast them as inner products of vectors and then apply the Schwartz inequality.

Limits on C_1:

$$C_1=\sum_i\Big|\sum_\mu a_{i\mu}\Big|^2=\sum_i\sum_\mu a_{i\mu}^*\sum_{\mu'}a_{i\mu'}.$$

We cast this expression in terms of a vector product by identifying $a_{i\mu}\to(\vec{A})_{i\mu}\sum_{\mu'}a_{i\mu'}\to(\vec{B})_{i\mu}$. Now applying the Schwartz inequality ($|\vec{A}\cdot\vec{B}|^2\leq A^2B^2$) we have

$$C_1^2\leq\sum_{i\mu}|a_{i\mu}|^2\sum_{i\mu}\Big|\sum_{\mu'}a_{i\mu'}\Big|^2\leq 4C_1,$$

therefore,

$$0\leq C_1\leq 4. \tag{9}$$

The limit $C_1=4$ occurs when $a_{i\mu}=a_{i\mu'}$. Since the $|i\mu\rangle$ are the sp^3 bonds, this corresponds to pure s states on the sites. The limit $C_1=0$ occurs when $\sum a_{i\mu}=0$, which corresponds to a pure p state.

Limits on C_2:

$$C_2=\sum_{i\mu}a_{i\mu}^*a_{i_\mu\mu}.$$

Setting $a_{i\mu}=A_{i\mu}$, $a_{i_\mu\mu}=B_{i\mu}$, we get

$$C_2^2\leq\sum_{i\mu}|a_{i\mu}|^2\sum_{i\mu}|a_{i_\mu\mu}|^2\leq 1,$$

therefore,

$$-1\leq C_2\leq 1. \tag{10}$$

These limits correspond to the bonding and antibonding configurations. The limits are reached for $a_{i\mu}=\pm a_{i_\mu\mu}$. As we shall see later, the sign of C_2 distinguishes the conduction and valence bands.

Limits on C_3: The limits on C_1 and C_2 can occur independently, but the limits on the other terms are related, as we shall see now:

$$C_3=\sum_{i\mu}a_{i\mu}^*D_{i\mu}+\sum_{i\mu}D_i^*a_{i_\mu\mu}-2C_2.$$

Defining $C_3'=C_3+2C_2$, we have

$$C_3'=2\sum_{i\mu}a_{i\mu}^*D_{i\mu}.$$

Making the identification $a_{i\mu}=A_\mu$, $D_{i_\mu}=B_\mu$, we get from the Schwartz inequality

$$C_3'^2\leq 4\sum_{i\mu}|a_{i\mu}|^2\sum_{i\mu}|D_{i_\mu}|^2\leq 4\times 4C_1\leq 64.$$

The limits occur when the vectors $\vec{A}$ and $\vec{B}$ are parallel or antiparallel and when $a_{i\mu}=a_{i\mu'}$. This is also the condition for C_2 to reach its limits and for $C_1=4$. We therefore have

$$-6 \leq C_3 \leq 6 . \tag{11}$$

Limits on E_4: The matrix elements discussed so far have been structure independent, so it has been straightforward to apply the Schwartz inequality. However, now we have to look at structure-dependent terms. We can study the limits of the energy for our wave function, but these "limits" may now be structure dependent and the exact limit may arise for a special configuration. The crystalline value of $V_4^{i,i\mu}=V_4^c$ is given by $V(\phi)=V(180°)$. From Fig. 7 we see that $V_4^{i,i\mu} \leq V_4^c$. Thus we may write

$$E_4 \leq V_4^c \sum_{i,\mu,\mu';\mu\neq\mu'} a_{i\mu}^* a_{i_\mu,\mu} \leq V_4^c, C_4 ,$$

where

$$C_4 = \sum_{i,\mu,\mu';\mu\neq\mu'} a_{i\mu}^* a_{i_\mu,\mu} .$$

We are now in a position to study the limits of C_4. Adding $\sum_{i\mu} a_{i\mu}^* a_{i_\mu\mu}$ to C_4 we get

$$C_{4'}=C_4+C_2=\sum_{i\mu,\mu'} a_{i\mu}^* a_{i_\mu,\mu} ,$$

thus removing the restriction $\mu\neq\mu'$.

We now associate vectors $(\vec{X})_1=X_1(a_{i1}, a_{i2}, \ldots)$ with each site. C_4' is then of the form

$$C_4'=\sum_{i,\mu} X_i X_{i_\mu} ,$$

where $X_i X_{i_\mu}$ contains the term $a_{i\mu}^* a_{i\mu\mu}$ and other terms arising from C_4. If there are no odd rings in the structure, i.e., if the structure is bichromatic, we can divide it into two substructures each containing the nearest neighbors of those sites on the other. This separation allows wave functions to have pure bonding or pure antibonding nature. We shall show later that the spectral limits for a mixed structure are associated with states confined to regions which are locally even. Introduction of odd rings causes a mixture of bonding and antibonding states such that the energy of the eigenfunctions moves away from the limits into the band. Thus for the purpose of studying the limits we can consider the wave function to be purely bonding or antibonding. It is useful to study the two cases where $\vec{X}_i$ and $\vec{X}_{i\mu}$ lie in the same "quadrant" or in the opposite "quadrant", since this corresponds to C_2 being positive or negative.

In the same-quadrant case, we see immediately that the lowest value of C_4' is zero. For the upper limit we use the Schwartz inequality

$$|C_4'|^2 \leq \sum_{i,\mu} |X_i|^2 \sum_{i\mu} |X_i|^2 \sum_{i\mu} |X_{i_\mu}|^2$$
$$\leq 16 \quad \text{as} \sum_i |X_i|^2 = 1 , \tag{12}$$

i.e., C_4' ranges from 0 to 4 in this case. Similarly in the opposite quadrant C_4' ranges from 0 to -4. Remembering the definition of C_4', the ranges of C_4 are -1 to 3 and -3 to 1 for C_2 positive and negative, respectively.

Limits on E_5 and E_6: The limits on the E_5 and E_6 terms can be obtained by arguments similar to the ones used above. The extremum values of V_5 and V_6 occur at $V_5^{i,i\mu}=V(60°)=V_5^c$ and $V_6^{i,i\mu}=V(0°)=V_6^e$, where the superscripts c and e stand for crystalline and eclipsed positions, respectively. Thus from Fig. 7 we have

$$|E_5| \leq |V_5^c| C_5 ,$$

where C_5 has the same structure as C_4 and will therefore have the same limits. Similarly, for E_6 we have

$$|E_6| \leq |V_6^e| C_6 ,$$

where the superscript e stands for the eclipsed position. Again C_6 has the same form as C_4 and C_5 and will have the same limits. Of course, the limits on C_4, C_5, and C_6 may not occur simultaneously.

From the above discussion it is clear that the E_4, E_5, and E_6 terms, though structure dependent, have well defined limits. This is a consequence of the disorder being only dihedral-angle disorder. It is useful to examine these limits to see what states they correspond to.

The $C_1=4$ limit arises when $a_{i\mu}=a_{i\mu'}$. It is easy to see that in this case the wave function is pure s. The limits $C_2=+1$ and -1 then give rise to bonding and antibonding limits, as shown in Fig. 8(a) and 8(b). The conditions for the limits on C_4, C_5, and C_6 are also satisfied simultaneously. In the limit $C_1=0$, remembering that our basis functions are the sp^3 orbitals, we see that this corresponds to pure p states.

As we have already mentioned, the V_1 and V_2 interactions are the strongest interactions and will be dominant in determining the limits of the spectra. We also note from the signs of V_1 and V_2 that when C_2 is positive, these two terms have the same sign while when C_2 is negative they oppose each other. This means that the on-site terms and the nearest-neighbor terms occur with the same sign in the bonding states and with opposite sign in the antibonding states. For the bonding case, we therefore expect the limits to arise from pure states, while for the anti-

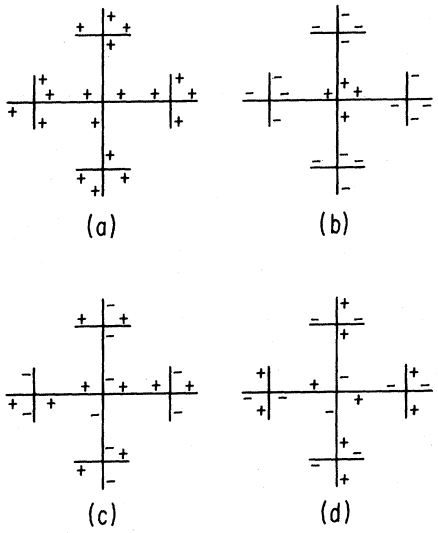

FIG. 8. (a) Configuration for the bonding s states. (b) Configuration for the antibonding s states. (c) Configuration for the bonding p states. (d) Configuration for the antibonding p states.

bonding case the limits may be from mixed states. We shall discuss this more clearly when discussing the conduction band.

V. THE VALENCE BAND

From Fig. 8 we realize that in moving from one site to the next the amplitude may or may not change sign. The latter case gives rise to lower energy states (V_2 is negative) which make up the valence band. Thus in the valence band we shall look at the positive values of C_2.

A. Bottom of the valence band

From Eq. (2) we know that V_1 is large and negative, so that we require the maximum positive value of C_1. The same is true for the V_3 term which is negative. Similarly V_2 is large and negative so that we require the maximum positive value of C_2. This choice automatically minimizes the V_3 term and fixes the values of the remaining C's. Since V_1 and V_2 dominate, we arrive at the minimum energy

$$E^V_{\min} = 4V_1 + V_2 + 6V_3 + 3(V_4 + V_5 + V_6). \tag{13}$$

We arrive at Eq. (13) because $V_4 + V_5 + V_6$ is invariant under dihedral-angle disorder. From Fig. 8(a), it is clear that this state corresponds to a bonding s state. We call this band edge a "normal bound". At this bound the wave function at each site is s type, i.e., $\psi_i = (1/2\sqrt{N})S_i$, where N is the number of sites in the system. Close to the bound we introduce the vector K and write the wave function as a perturbation series in K:

$$\begin{aligned}
\psi_i &= \frac{1}{2\sqrt{N}}\,(\alpha_i S_i + \beta_i P_i)\exp(i\chi_i),\\
\alpha_i &= 1 + a_i^{(1)}K + a_i^{(2)}K^2 + \cdots,\\
\beta_i &= b_i^{(1)}K + b_i^{(2)}K^2 + \cdots,\\
\chi_i &= \vec{K}\cdot\vec{r}_i + \phi_i,\\
\phi_i &= \tau_i^{(1)}K + \tau_i^{(2)}K^2 + \cdots.
\end{aligned} \tag{14}$$

The energy close to the edge (small K) is given by

$$E = \frac{1}{4N}\Bigg[\sum_{ii_\mu} E_{ss}(0) + E_{ss}(\tfrac{1}{2}) + K\sum_i\Bigg(\sum_{i_\mu} iE_{ss}(\tfrac{1}{2})(\vec{r}_{ii_\mu} + \tau_{ii_\mu}) + \sum_{i_\mu} E_{ss}(\tfrac{1}{2})(a_i^{(1)} + a_{i_\mu}^{(1)}) + E_{sp}(\tfrac{1}{2})(b_i^{(1)} + b_{i_\mu}^{(1)})\Bigg)$$

$$+ K^2\sum_i\Bigg(\sum_{i_\mu} E_{ss}(\tfrac{1}{2})(a_i^{(2)} + a_{i_\mu}^{(2)}) + E_{sp}(\tfrac{1}{2})(b_i^{(2)} + b_{i_\mu}^{(2)}) + E_{pp}(\tfrac{1}{2})(b_i^{(1)} + b_{i_\mu}^{(1)}) + \cdots\Bigg)\Bigg].$$

For purely dihedral-angle disorder, $\sum_{i_\mu}(\vec{r}_{ii_\mu} = \vec{r}_i - \vec{r}_{i_\mu})$ is zero, so that for real energies $\sum_{i_\mu}(\tau_{ii_\mu} = \tau_i - \tau_{i_\mu}) = 0$. Since $E(\psi = s)$ is a minimum, the terms proportional to K are zero, so that $a_i^{(1)} = b_i^{(1)} = 0$. To order K^2, the energy contains only invariant terms $E_{ss}(\frac{1}{2})$ and $E_{sp}(\frac{1}{2})$, so that the edge is crystalline-like, with deviations appearing in order K^3 where the noninvariant term $E_{pp}(\frac{1}{2})$ appears.

B. Top of the valence band

The top of the valence band is affected by the dihedral-angle variations in a very interesting manner. To get as high in energy as possible one would like $C_1 = 0$. Together with $C_2 = 1$ this implies $C_3 = 2$. However, the remaining terms in the energy are structure dependent. We note that V_4 is positive and V_5 and V_6 are negative. To get

the highest energy we therefore want C_4 to be positive and large and C_5 and C_6 to be negative and large. From the discussion of Sec. VII this gives us $C_4=3$, $C_5=-1=C_6$. Also since $V_4^c \geq V_4^{i,i_\mu}$, and $|V_5+V_6|^c \geq |V_5+V_6|^{i,i_\mu}$, the limit is

$$E^v_{\max}=V_2+2V_3+3V_4^c-V_5^c-V_6^c \tag{15}$$

which is the energy of the $\Gamma_{25'}$ point in the crystal.

To find variationally the maximum energy of an extended state, we choose a configuration for the a_{i_μ} given by the crystalline value. This will give a lower limit to the actual energy of an extended state and will be a lower limit to the mobility edge. The energy may be written as

$$E^v_{\max}(\phi)=\sum_i E^v_{\max}(\varphi_i),$$
$$E^v_{\max}(\phi_i)=\sum_{i_\mu} E^v_{\max}(\phi_{i,i_\mu}) \tag{16}$$
$$=\frac{1}{4N}\sum_{i_\mu}[V_2+2V_3+3V_4(\phi_{i,i_\mu})-V_5(\phi_{i,i_\mu})-V_6(\varphi_{i,i_\mu})],$$

where ϕ_{i,i_μ} gives the dihedral angle between the sites i and i_μ. If $\Delta\phi$ is the change in the dihedral angle from the crystalline value, from Eq. (12) we have

$$V_4(\Delta\phi)=0.3-\sin^2\Delta\phi/2,$$
$$V_5(\Delta\phi)=0.3-\cos^2(30^\circ-\Delta\phi/2),$$
$$V_6(\Delta\phi)=0.3-\cos^2(30^\circ+\Delta\phi/2),$$

so that

$$E^v_{\max}(\phi_{i,i_\mu})=\frac{1}{4N}\sum_{i_\mu}(V_2+2V_3+0.3+1.5\cos\Delta\phi_{i,i_\mu}). \tag{16'}$$

The maximum is reached for the crystalline structure as we found earlier. The problem is similar to the Lifshitz alloy problem,[22] except that instead of two components A and B, we now have a continuous distribution, the ends of which correspond to the staggered and eclipsed cases. Localized states will exist near the top of the valence band as in the case of the Lifshitz alloy problem. An estimate of the width of the tail of localized states can be obtained from Eqs. (16), (16′), and (1):

$$\overline{W}=E^v_{\max}-\overline{E^v_{\max}(\phi)}$$
$$=E^v_{\max}-\int P(\phi)E^v_{\max}(\phi)d\phi\cong 0.3 \tag{17}$$

expressed in eV. This is an upper limit to the tail width as discussed earlier and is a good estimate of the magnitude of the tail width due to dihedral-angle disorder.

C. First peak of the valence band

The valence band of the crystalline silicon has three main features denoted by the peaks I, II, and III in Fig. 1(a). Peak I is primarily due to πp states. The tetrahedral symmetry of silicon assures that the mixing of s states with πp states is very small. For example, if one assumes a $\vec{k}$ vector given by $\vec{k}=k(a,b,0)$, then it is simple to see that

$$\sum_{nn}\langle s|H|p\pi\rangle \propto E_{sp\sigma}[(a-b)\sin k(a+b)+(a+b)\sin k(b-a)]. \tag{18}$$

Similar results are obtained for any general direction. Thus along the symmetry direction there is no s-$p\pi$ mixing. In a general direction away from the symmetry axes the mixing is proportional to $k_\perp^3$ where $k_\perp$ is the component of $\vec{k}$ perpendicular to the nearest symmetry axis. Thus the transverse p states combine primarily with each other to form the peak I. With dihedral-angle disorder each stom is still surrounded by a perfect tetrahedron so that we expect the peak I to be still made from transverse p states. In the amorphous state, the width of peak I reduces and the edge close to the top of the valence band becomes steeper as shown in Fig. 1. Joannopoulos and Cohen[9] studied various crystalline forms of silicon to understand these features and concluded that they were due to bond-angle variations. However, it is not clear why bond-angle variations, which change the tight-binding (TB) matrix elements, make the edge steep. Also, in the various structures studied there are other parameters, e.g., dihedral angles, which vary.

We find that the dihedral-angle variations are primarily responsible for the features observed in the peak I in the amorphous state. Near the top of the valence band there is a redistribution of states. As discussed above these states are confined to regions where $\Delta\phi\sim 0$. Such regions which are spherical in shape dominate the tail.[12] The highest energy of a state is given by[22]

$$E=E_v+\frac{2\pi^2\hbar^2}{m^*V^{2/3}}, \tag{19}$$

where V is the volume (in which $\Delta\phi\sim 0$) in which the state is confined and m^* is the effective mass.

Clearly the edge E_v will be reached with zero probability in the disordered structure (here $m^* < 0$). If we assume as Lifshitz did that the probability to find a volume V which is "crystalline-like" goes as $\exp(-cV)$, where c is a constant, then the density of states near the edge is given by[22]

$$n(E) \propto \exp\left[-\left(\frac{E-E_v}{E_0}\right)^{-3/2}\right]. \quad (20)$$

States near the top of the valence band in the crystalline silicon are affected substantially by dihedral-angle disorder. In general they are pushed in to the band according to the arguments above. Deeper in the band (for energies more than 0.3 eV below the top of the valence band) not much change is expected, so that in general the change shown in Fig. 9 is expected for the density of states. The combination of the valence-band top appearing as a Lifshitz limit and the appearance of a tail of localized states are responsible for the sharpening of the valence-band edge and the upward shift of the maximum of peak I in going from the crystalline to a-Si. From the nature of our arguments we expect these results to hold for other tetrahedral semiconductors also as long as the sp^3 orbtials are the atomic functions giving rise to the band structure. The above results are qualitative in nature and it is difficult to get a simple quantitative estimate of the precise shape of the valence-band edge.

One can understand the results at the top of the valence band as follows. In the crystal the top is reached by putting p_x (or p_y or p_z) functions on each site, so that the energy involves only $E_{xx}(\frac{1}{2},\frac{1}{2},\frac{1}{2})$ term. Any change from this introduces $E_{xy}(\frac{1}{2},\frac{1}{2},\frac{1}{2})$ term which lowers the energy. In the dihedrally disordered structure it is not possible to put p_x functions on each site, so that the extended state will always have $E_{xy}(\frac{1}{2},\frac{1}{2},\frac{1}{2})$ terms, thus lowering the energy of the state below the crystalline limit. The crystalline limit can thus be approached only by localized states in which the wave function is confined to large, improbable regions of the amorphous structure within which the structure is essentially crystalline.

VI. THE CONDUCTION BAND

As discussed briefly in Sec. VII, the fact that the states in the conduction band are antibonding forces the on-site and nearest-neighbor interactions to give opposing contributions to the energy. This leads to the possibility that the bottom of the conduction band is not due to a pure state. It is therefore not possible to apply as simple a method as used for the valence band. We use, therefore, a less rigorous approach which is only suggestive of what one may expect upon introduction of dihedral-angle disorder.

Let us study the limits of the conduction band in a crystal and understand the differences between silicon and germanium. A general wave function is $\sum_i(a_i s_i + \vec{b}_i \cdot \vec{p}_i)$, where $\sum_i |a_i|^2 + |b_i|^2 = 1$. The relative signs of a_i and a_{i_μ}, $\vec{b}_i$ and $\vec{b}_{i_\mu}$ (i and i_μ are nearest neighbors) determine whether the energy of the state lies in the conduction or valence band. Figure 10 shows the on-site and nearest-neighbor contributions to the energy as the nature of the wave function goes from pure s to pure p in the conduction band (we only look at the bottom of the conduction band). The on-site contribution is determined uniquely by the $|a|$ and $|b|$. However the nearest-neighbor contribution depends on the direction of $\vec{b}$ as well. In general the energy will contain terms $E_{ss}(\frac{1}{2})$, $E_{xx}(\frac{1}{2})$, $E_{sx}(\frac{1}{2})$, $E_{xy}(\frac{1}{2})$ using the Slater-Koster notation. A wave function of the form $\psi = \sum_i a_i |s_i\rangle + \vec{b}_i(1,0,0)\cdot\vec{p}_i$ involves no $E_{xy}(\frac{1}{2})$ term, while $\psi = \sum_i a_i s_i + \vec{b}_i(1,1,1)\cdot\vec{p}_i$ involves a large $E_{xy}(\frac{1}{2})$ term in general. Thus the direction of $\vec{b}$ essentially determines the relative mixture of E_{xx} and E_{xy} terms or of the $pp\sigma$ and $pp\pi$ interactions (for a fixed sp mixture). Thus the relative strength of the $pp\sigma$ and $pp\pi$ interactions determines which kind of wave function will form the conduction-band minimum. As is well known, in silicon the minimum is given by a wave function for which $\vec{b}$

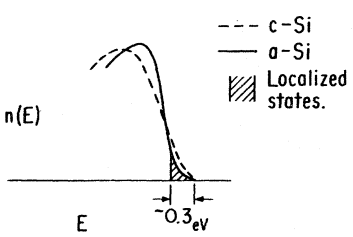

FIG. 9. Sketch of the effect of the dihedral-angle disorder on the density of states $n(E)$ near the top of the valence band.

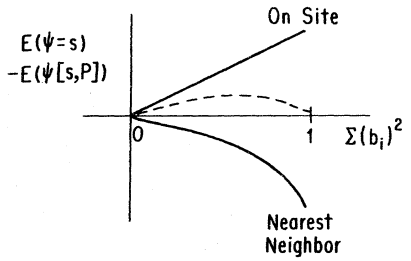

FIG. 10. Energy difference between a pure s state and a mixed state for on-site and nearest-neighbor terms in the conduction band.

$=\vec{b}(1,0,0)$, while for germanium it is given by $\vec{b}=\vec{b}(1,1,1)$. For dihedral-angle disorder the relative strengths of the σ and π interactions are not altered, so that the character of the wave functions forming the minimum is not expected to change. It is possible, though, that the wave function may not be compatible with the structure or may be able to exist only in particular regions of the structure, as happened at the top of the valence band.

For silicon the bottom of the conduction band is near X_1 (in the crystal). At X_1, the wave function is effectively s (or p_x) at one site and p_x (or s) at the neighboring site. Due to this fact the energy at X_1 involves the invariants V_1, V_2, V_3, and $(V_4+V_5+V_6)$, or only σ-type interactions. We thus expect very small fluctuations near the bottom of the conduction band in a-Si arising from dihedral-angle disorder. This is not the case for germanium, for which the bottom of the conduction band involves a substantial π interaction.

We find in this simple picture that in a-Si the valence-band top has a tail of localized states ~ 0.3 eV in width, while the conduction-band edge is essentially free of localized states (Fig. 11). In germanium, however, we expect both the valence-band and the conduction-band edges to have similar widths for their tails of localized states.

VII. TOTAL EFFECT OF QUANTITATIVE DISORDER

In this section we combine what we have found in the previous sections and compare it with some known experimental results. We notice first that dihedral-angle disorder is primarily responsible for the sharpening and shift of the valence-band edge. The bond-angle and bond-length disorder will smear this shape further as shown in Fig. 11. From the above results we expect the total energy fluctuations near the top of the valence band to be ~ 0.5 eV and at the conduction-band edge to be ~ 0.2 eV. These represent an upper limit to the widths of the tails of localized states.

An actual calculation for the amorphous structure is extremely difficult. Hama and Yonezawa[23] have studied the effect of quantitative disorder using coherent-potential-approximation (CPA) techniques. The amorphous structure is represented by a Weaire-Thorpe Hamiltonian with random V_1 and V_2 terms. The disorder was then varied to find how much was required to merge the peaks II and III as observed in the x-ray photoemission spectroscopy (XPS) results. They found that Lorentzian half-widths of ~ 2 eV were required. Such a large disorder would also put a high density of localized states in the band gap which would be inconsistent with the narrow observed tails. We find that the structural models of a-Si and our calculations predict an order-of-magnitude-lower quantitative disorder compared to what is required by them to explain the XPS results for peaks II and III. Our estimate is consistent with the narrow tails of localized states and the observed shape of peak I. In the next section we describe another source of disorder which is expected to be present in amorphous semiconductors, which we consider responsible, together with the dihedral-angle disorder for the merging of peaks II and III.

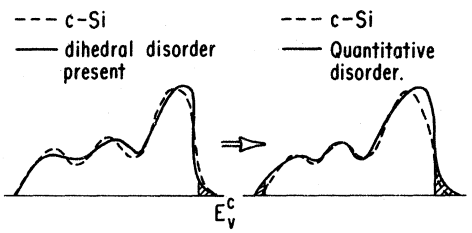

FIG. 11. Effect of only dihedral-angle disorder (left) and total quantitative disorder on the density of states in the valence band of silicon.

VIII. TOPOLOGICAL DISORDER

In addition to the obvious quantitative disorder, another kind of disorder present in amorphous semiconductors is the topological disorder. The primary manifestation of topological disorder is in the ring statistics of the structure. In the crystalline structure the ring statistics is even, but in the general CRN we expect both odd and even rings to be present. The role of odd rings in merging of the peaks II and III has been pointed out.[9] The introduction of localized states due to topological disorder was demonstrated by Cohen, Singh, and Yonezawa.[21] These reuslts will be briefly discussed here and the results for a more complete Hamiltonian as chosen here will be inferred from them.

The Hamiltonian for the s-band model is

$$H=\sum_{i\mu}|i\rangle V\langle i_\mu|\,, \tag{21}$$

where V is hopping matrix element between the nearest-neighbor sites i and i_μ and will be assumed negative. The Weaire-Thorpe model can be mapped on to the s-band model.[6] The energy for a wave function $\psi=\sum_i a_i S_i$ is

$$E=ZVC,\ ZC=\sum_{i,\mu} a_i^* a_{i_\mu} - 1 \leq C \leq 1\,. \tag{22}$$

At the lower bound the eigenfunction is bonding, $a_i=N^{-1/2}$, where N is the number of sites. It has

been shown that this bound is a normal bound[21] in the sense that the density of states has a form

$$n(E) \propto (E - ZV)^{1/2}, \tag{23}$$

similar to the crystalline-band edge. No localized states are expected at this edge, and only a small correction is expected for the effective mass near the edge.

The upper bound, which is an antibonding bound, has a different behavior. This bound is reached for the amplitude variation $a_i = \pm N^{1/2}$ and $C = -1$. Such a state which changes sign across each bond is incompatible with a mixed structure having both even and odd rings. Thus a state of this property cannot extend to the entire structure. If ν is the minimum possible number of frustrated bonds, i.e., bonds across which the sign change is not possible due to the presence of odd rings, the above type of antibonding state has a maximum expectation value of the energy

$$E_{op} = -(Z - 4\nu/N)V, \tag{24}$$

which is like an optical potential. States near or above E_{op} are expected to be drastically affected by the disorder.

Rivier[24] has shown that odd-membered rings can be threaded by a continuous line which avoids even rings and either closes in a loop or ends at the surface. The odd rings are therefore associated with randomly fluctuating densities of defects in an even structure. One can imagine regions free of odd rings. The problem is similar to the Lifshitz alloy problem,[22] and the antibonding bound is reached with zero probability. States near this bound are localized states confined to regions free of odd rings. We assume as was done by Lifshitz that if c is the concentration of even rings, the probability of finding a volume V free of odd rings is proportional to $\exp(-cV)$. The density of states near the antibonding limit is then given by

$$n(E) = n_0 \exp\{-[E_a/(-ZV - E)]^{3/2}\}, \tag{25}$$

with n_0 and E_a constants. States close to the antibonding limit in the crystalline case are now pushed into the bulk of the band. Conservation of the first moment of the density of states results in a peak in the density of states as shown in Fig. 12. It has been pointed out that the mobility edge will lie above the variationally determined energy E_{op}.

It was shown by Weaire and Thorpe[6] that their model could be mapped onto an s-band model. A more complete model such as we have used causes the δ functions observed in the Weaire-Thorpe model to broaden into the peak I, but peaks II and III are qualitatively similar to the

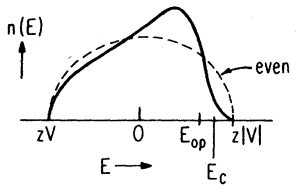

FIG. 12. Effect of topological disorder on the density of states of the s-band model. Dotted line: crystalline case; dark line: disordered case; E_c: mobility edge.

ones obtained from the Weaire-Thorpe model. Thus the s-band-model results can be used to understand the effects of topological disorder on these peaks. It is easy to see that the symmetry properties of p-bonding states is similar to those of the s-antibonding states. Thus the states in the upper half of the valence band containing p-bonding states will be pushed down into the band due to the presence of odd rings. The transverse p states forming the peak I will be unaffected by the odd rings as in the case of the Weaire-Thorpe model.

A rough estimate of the lower limit on the concentration of odd rings can be obtained from the XPS results and our discussions. The difference between properly normalized XPS results for the crystalline and amorphous structure gives the net displacement of the density of states due to disorder. Separating the states into π (peak I) and σ (peaks II and III), we get an estimate for the displacement of the density of states due to topological disorder. Assuming that states move from near the top of the valence band to fill the valley between peaks II and III, we can estimate the energy E_{op} discussed earlier. Using the transformation between the s-band model and the sp^3 Weaire-Thorpe model, we can determine ν defined in Eq. (24). This comes out to be ~12%. Considering the simplicity of the arguments this is in good agreement with the values obtained by actual construction of CRN's.[25]

The bottom of the conduction band is reached by a wave function in which s and p functions are placed alternately on the atomic sites. The effect of the frustration due to the odd rings is felt most at the energies corresponding to a wave functions which are s antibonding or p bonding, as discussed earlier. In the case of a mixed wave function as is the case at the bottom of the conduction band, the effect is rather small. The effect can be studied variationally and it is seen that essentially for an odd ring the $E_{sx}(\frac{1}{2})$ matrix element is replaced by $E_{ss}(\frac{1}{2})$. Assuming a 12% odd ring concentration, the variational shift is about 0.1 eV. It has been suggested that the odd-even disorder may not be present in amorphous

films made from III-V compounds.[26,27] The strong energy couplings between atoms of different kinds are expected to force each atom to be surrounded by atoms of the other kind. This will minimize the odd-even disorder and will lead to amorphous films of better quality.

IX. CONCLUSIONS

We find from the study in this paper that a simple tight-binding scheme is capable of giving very interesting results for a-Si. We find that the quantitative disorder is rather small in this material and produces narrow tails of localized states. The dihedral-angle disorder is a primary importance near the top of the valence band, and understanding it is crucial to the preparation of better amorphous films, especially with better hole properties. The topological disorder is of prime importance near the bottom of the conduction band in a-Si. We find the dihedral-angle disorder explains the changes observed in peak I in going from the crystalline to the amorphous state, while the topological disorder is mainly responsible for the merging of peaks II and III.

Our aim in this paper was not to do rigorous calculations for amorphous semiconductors, in view of the difficulty involved. We found, however, that much information about the disordered state could be achieved through the intuitive and semiquantitative methods used here. We find that the nature of the wave functions near the band edges in the crystal is rather important in determining the "quality" of the corresponding edge in the amorphous state. By quality we mean the extent of localization present near the mobility edge. We have also been able to study the relative roles of different disorders present in the amorphous state modeled as a continuous random network. Our results reinforce the idea that the local environment in the amorphous structure is important in forming the band limits. However, the somewhat longer-range order which determines the dihedral-angle distribution and ring statistics of the structure is also very crucial, especially in determining the localized states near the band edges. These results allow us to understand the origin of the localized states in different amorphous semiconductors, e.g., we find that while dihedral-angle disorder is not so important for the conduction-band edge of a-Si, it is very important for the conduction-band edge of a-Ge in which the dihedral-angle disorder may produce tails of localized states with widths ~ 0.3 eV. Such information is important for preparation of better amorphous films. We find for example that silicon is intrinsically better than germanium as far as dihedral-angle disorder is concerned and that III-V compounds can produce high-quality amorphous films.

Here we have ignored the role of the d levels. Inclusion of these levels may not only improve the crystalline band structure, but may also give a more accurate picture for the amorphous state. We have examined the dihedral-angle disorder in context of nearest-neighbor interactions alone. Inclusion of second-neighbor interactions may introduce important effects, since now the local atomic configuration will no longer be constant.

ACKNOWLEDGMENTS

I am very grateful to Professor M. H. Cohen who was a constant source of ideas and encouragement. I also gratefully acknowledge valuable discussions with Professor F. Yonezawa and Professor H. Fritzsche. This research was supported by the Materials Research Laboratory Program of the National Science Foundation at the University of Chicago. The author is grateful for a General Electric Foundation Fellowship.

---

*Presented as a thesis to the Department of Physics, the University of Chicago, in partial fulfillment of the requirements for the Ph.D. degree.

†Present address: Department of Material Science, University Park, Los Angeles, CA 90007.

[1]W. E. Spear and P. G. Lecomber, Philos. Mag. 33, 937 (1976).

[2]A. Madan and S. R. Ovshinsky, J. Non-Cryst. Solids 35–36, 171 (1980).

[3]L. Ley, S. Kowalczyk, R. Pollak, and D. A. Shirley, Phys. Rev. Lett. 29, 1088 (1972).

[4]D. T. Pierce and W. E. Spicer, Phys. Rev. B 5, 3017 (1972).

[5]D. Weaire and M. F. Thorpe, Phys. Rev. B 4, 2508 (1971).

[6]D. Weaire and M. F. Thorpe, Phys. Rev. B 4, 3518 (1971).

[7]M. Kelly and D. Bullett, J. Non-Cryst. Solids 21, 155 (1976).

[8]W. Y. Ching, C. C. Lun, and L. Guttman, Phys. Rev. B 16, 5488 (1977).

[9]J. D. Joannopoulos and M. L. Cohen, Phys. Rev. B 7, 2644 (1973).

[10]J. D. Joannopoulos, Phys. Rev. B 16, 2764 (1977).

[11]J. Ziman, J. Phys. C 4, 3129 (1971).

[12]M. H. Cohen, J. Singh, and F. Yonezawa, J. Non-Cryst. Solids 35–36, 55 (1980).

[13]J. C. Slater and G. F. Koster, Phys. Rev. 94, 1498

(1954).
[14]J. Chelikowsky and M. L. Cohen, Phys. Rev. B 10, 5095 (1974).
[15]D. E. Polk, J. Non-Cryst. Solids 5, 365 (1971).
[16]L. Guttman, Bull. Am. Phys. Soc. 22, 64 (1977).
[17]G. A. Connell and R. J. Temkin, Phys. Rev. B 9, 5323 (1974).
[18]C. Herring and E. Voigt, Phys. Rev. 101, 944 (1956).
[19]R. M. Martin and H. Wendal, Solid State Commun. 22, 21 (1977).
[20]J. H. Davies, J. Non-Cryst. Solids 35–36, 67 (1980).
[21]M. H. Cohen, J. Singh, and F. Yonezawa (unpublished).
[22]I. M. Lifshitz, Adv. Phys. 13, 483 (1964).
[23]T. Hama and F. Yonezawa, Solid State Commun. 29, 371 (1979).
[24]N. Rivier, Philos. Mag. A40, 859 (1979).
[25]D. Beeman and B. L. Bobbs, Phys. Rev. B 12, 1399 (1975).
[26]J. D. Joannopoulos and M. L. Cohen, Phys. Rev. B 10, 1545 (1974).
[27]M. H. Cohen, H. Fritzsche, J. Singh, and F. Yonezawa (unpublished).